Picomolar Detection of Protease Using Peptide/Single Walled Carbon Nanotube/Gold Nanoparticle-Modified Electrode

Khaled A. Mahmoud,[†] Sabahudin Hrapovic,[†] and John H. T. Luong[†,‡,*]

[†]Biotechnology Research Institute, National Research Council Canada, Montreal, Canada H4P2R2, and [‡]Department of Chemistry, University College Cork, Cork, Ireland

ABSTRACT Picomolar electrochemical detection of human immunodeficiency virus type-1 protease (HIV-1 PR) using ferrocene (Fc)-pepstatin-modified surfaces has been presented. Gold electrode surface was modified with gold nanoparticles (AuNP) or thiolated single walled carbon nanotubes/gold nanoparticles (SWCNT/AuNP). Thiol-terminated Fc-pepstatin was then self-assembled on such surfaces as confirmed by Raman spectroscopy and scanning electron microscope. The interaction between the Fc-pepstatin-modified substrates and HIV-1 PR was studied by cyclic voltammetry and electrochemical impedance spectroscopy. Both electrode materials showed enhanced electrochemical responses to increasing concentrations of HIV-1 PR with shifting to higher potentials as well as decrease in the overall signal intensity. However, the sensing electrode modified with thiolated SWCNTs/AuNPs showed remarkable detection sensitivity with an estimated detection limit of 0.8 pM.

KEYWORDS: protease · ferrocene-pepstatin inhibitor · carbon nanotubes · gold nanoparticles · biosensor

Protease, a critical component in mammalian cells and tissues, occurs naturally in all organisms and constitute 1%−5% of the gene content for various metabolic processes. This important enzyme is involved in a multitude of physiological reactions from simple digestion of food proteins to highly regulated cascades. Proteases have been used in various forms of therapy: oncology, inflammatory conditions, blood rheology control, and immune regulation. Proteases are also implicated in many viral and infectious diseases, for example, HIV-1 protease (HIV-1 PR), an aspartic protease that functions to cleave the nascent polyproteins synthesized during the viral replication cycle.[1−3] Consequently, intensive efforts have been directed toward the search for novel protease inhibitors with improved bioavailability, antiviral potency, and activity toward drug-resistant mutant viruses.[4−6] Protease inhibition renders the virus noninfectious as the body rapidly clears immature virions. However, owing to the high viral mutation rates, a single amino acid change within HIV-1 PR can render it invisible to an inhibitor, the active site of this enzyme can change rapidly when under the selective pressure of replication-inhibiting drugs. Thus, there is a critical need for high-throughput and sensitive protocols for detecting protease activity and/or screening potential protease inhibitors. In addition, the effect of binding various inhibitors on the protease structure is currently the focus of intensive research.[7−9] Although a plethora of different methods has been developed for detecting protease activity,[10−17] fluorescent methods are predominant.[18−23] However, fluorogenic methods require laboratory-based equipment, whereas other techniques require overnight incubation times. Recently, peptide-modified optical filters for detecting protease activity with a detection limit of 37 nM have been reported.[24]

Integration of metallic nanoparticles (NPs) with carbon nanotubes (CNTs) has attracted much interest because of the low resistance ohmic contacts of these composites.[25,26] Of particular interest is the attachment of gold NPs to the side walls of CNTs to fabricate highly efficient sensor devices.[27,28] CNT and gold NP-modified electrodes have many advantages such as high surface area, favorable electronic properties, ease of biomolecule attachment, and electrocatalytic effects.[29−32] Ferrocence (Fc)-peptide conjugates bound to gold electrodes,[33] allows for identifying and screening of HIV-1 PR in physiological conditions with a detection limit (LOD) of 1 nM.[34]

This paper describes an ultrasensitive electrochemical procedure that is more amenable to applications in the field and array format. A new strategy is engineered

*Address correspondence to John.Luong@cnrc-nrc.gc.ca.

Received for review February 7, 2008 and accepted April 01, 2008.

Published online April 18, 2008.
10.1021/nn8000774 CCC: $40.75

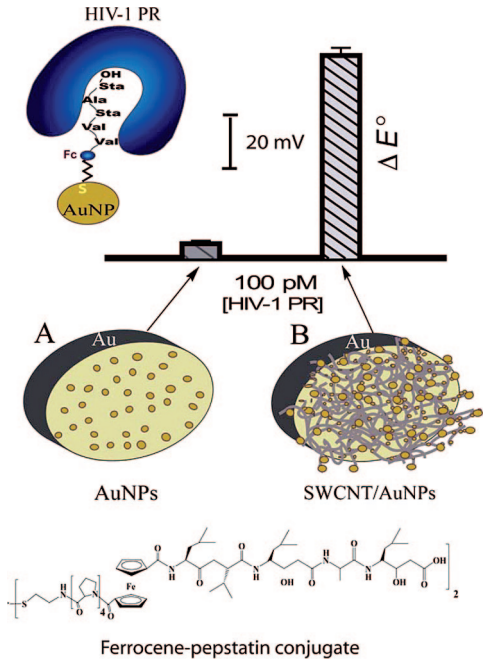

Figure 1. Schematic representation of the two detection protocols for HIV-1 PR using Fc-pepstatin modified surfaces: (A) AuNP and (B) SWCNT/AuNP-modified gold electrodes at 100 pM of the enzyme.

for the detection of HIV-1 protease (HIV-1 PR) by utilizing a gold NP-CNT-modified electrode to attain unprecedented detection sensitivity below the picomolar (pM) level (Figure 1). We advocate the use of pepstatin, a well-known potent inhibitor of aspartyl proteases. This hexa-peptide (Iva-Val-Val-Sta-Ala-Sta) has an unusual amino acid, statine or (3*S*,4*S*)-4-amino-3-hydroxy-6-methylheptanoic acid. It was first isolated from *Actinomyces*[35] because of its ability to inhibit pepsin at low concentrations.[36] Indeed, it inhibits nearly all acid proteases with high potency and has become a valuable research tool as well as a common constituent of protease inhibitor cocktails.

RESULTS AND DISCUSSION

Initially, we attempted to introduce gold NPs to the gold electrode surface (Figure 1) aiming for high detection sensitivity, the approach described by Li *et al.*[37] for DNA-binding cancer drugs. Gold NPs were deposited from a 0.5 M H_2SO_4 solution containing 5 mM $HAuCl_4$ using chronoamperometry at $E_r = 0.2$ V *versus* Ag/AgCl for 10 s. Under this condition, $AuCl_4^-$ was reduced to AuNPs. The cystamine containing Fc-pepstatin conjugate was self-assembled on the gold surface *via* Au−S bonding[38,39] and followed by the binding of increasing concentrations of HIV-1 PR as described in the Experimental Section. This setup allows Fc to be in close proximity to the electrode surface and thus unaffected by diffusive processes. Moreover, the communication between the recognition sequence and electrode surface would not be blocked by the binding event.[33] The electrochemical response of the films was evaluated by cyclic voltammetry (CV) measurements in an HIV-1 PR activation buffer at pH 4.7 containing 2 M $NaClO_4$ as the supporting electrolyte.

Figure 2 illustrates the formal potential ($E°$) change of the Fc probe as a function of the enzyme concentration. The films displayed a reversible one-electron redox peak with $E° = 0.486 \pm 0.005$ at 0.1 V/s *versus* Ag/AgCl. A linear relationship between the peak current i_{pc} and the scan rate indicated an adsorption controlled process (Figure S1, Supporting Information). Upon the selective binding of HIV-1 PR to the surface bound inhibitory peptide (Fc-pepstatin), a shift to higher potential together with a decrease in the peak current intensity was observed; indicating that the oxidation of the Fc group became increasingly difficult. Evidently, the bound enzyme was capable of blocking the penetration of the supporting electrolyte to the electrode surface, thereby decreasing its ability to oxidize Fc. At 0.5 nM enzyme concentration, only a slight decrease of the current intensity and a negligible shift in the formal potential was observed. This could be attributed to the limitation of the biosensor to register any binding activity at such a low concentration. $\Delta E°$ *versus* enzyme concentration was linear over the 0.5−10 nM range. Beyond the upper enzyme level, the response became nonlinear, indicating the saturation of the enzyme binding to the maximum protease inhibitor that could be loaded on the electrode surface. The LOD was 0.08 nM, estimated from $3(S_b/m)$, where S_b is the standard deviation of the measurement signal for the blank and m is the slope of the analytical curve in the linear region.[40] This detection limit was over 10-fold lower than the previously reported value (1 nM).[34]

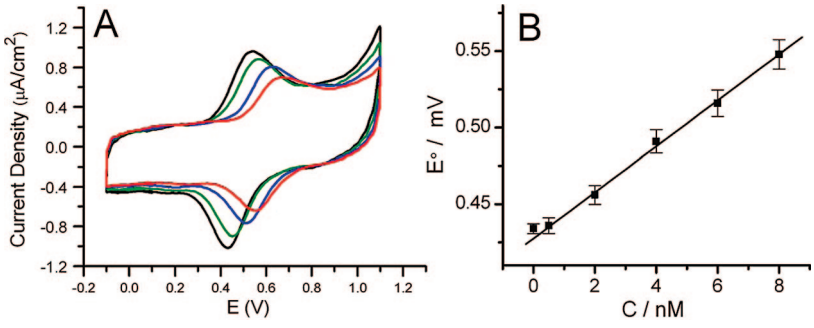

Figure 2. (A) Cyclic voltammogram of AuNP-modified gold electrode modified with Fc-pepstatin conjugate in the presence of increasing concentrations of HIV-1 PR: 0 (black, control), 0.5 (green), 4 (blue), and 8 nM (red); (B) Linear relationship between HIV-1 PR concentration and the formal potential $E°$. The assay buffer consisted of 0.1 M sodium acetate, 2 M $NaClO_4$, 1 mM EDTA, 1 mM DTT, 10% DMSO, pH 4.7. The $E°$ of the Fc/Fc^+ couple under the experimental conditions is 448 (±5) mV.

A series of experiments was conducted to improve the LOD by introducing aligned carbon nanotubes (ACNTs) as electrode material. Gold nanoparticles were deposited electrochemically on the outer walls of ACNTs

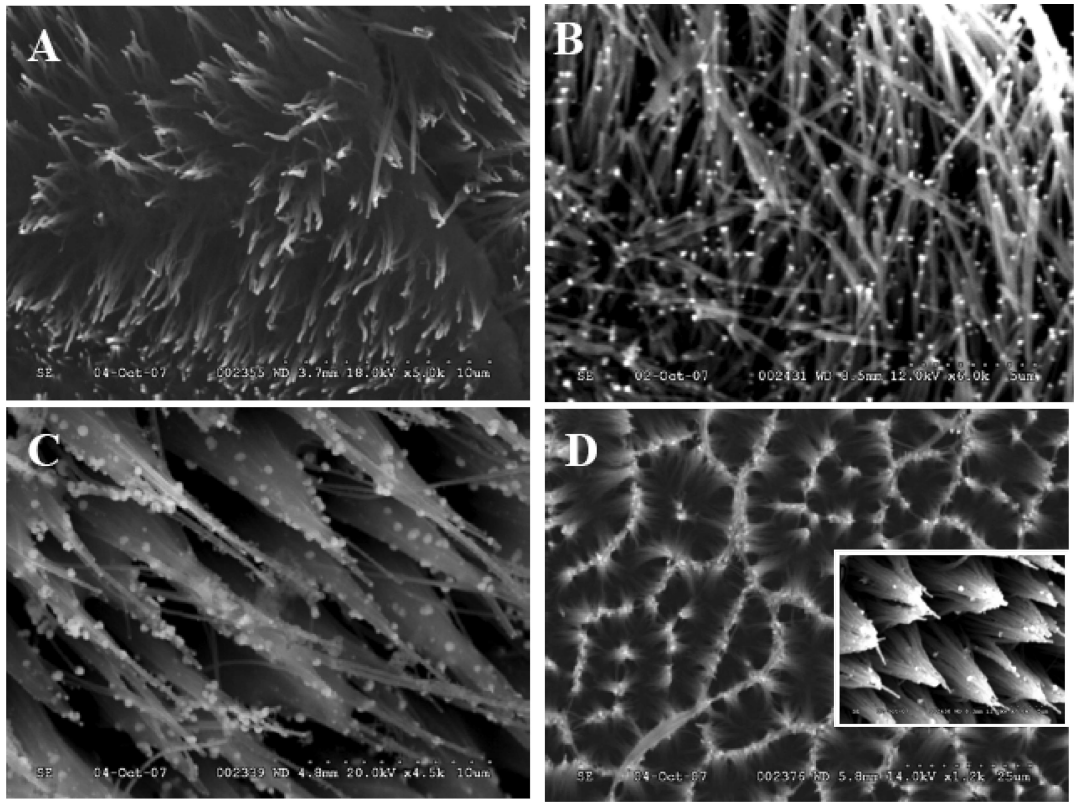

Figure 3. SEM images of (A) pristine aligned CNTs (5000×), (B) AuNP modified aligned CNTs (6000×), (C) peptide/AuNP/ aligned CNTs (4500×), and (D) protein/peptide/AuNP/ aligned CNTs (1200×). The inset in D shows AuNPs observable only at higher magnification (7000×). Only minimum bending of aligned CNTs was observed upon their rinsing under mild water stream (A) and drying under an argon stream. The Au nanoparticles deposition process (B) introduced additional stress but the nanotube array still consisted of individual tubes although with more bended morphology. Peptide binding (C) and protein adsorption step (D) exerted an additional pressure on the array and tubes were grouped together forming interesting patterns (D).

to facilitate the self-assembly of the peptide probe. The Fc-pepstatin film was self-assembled as described above and allowed to interact with HIV-1 PR. The binding of HIV-1 PR to the peptide modified electrode was confirmed by SEM micrographs. Upon binding with the HIV-1 PR, the morphology of ACNTs changed from aligned strands (Figure 3A) to ordered aggregates of several tubes (Figure 3D). This was not observed by washing the tubes with the assay buffer in the absence of HIV-1PR. The electrochemical response was monitored by CV (data not shown). However, the LOD of this system (~0.1 nM) was only comparable to the gold nanoparticle-modified electrode as discussed earlier. Notice also that when 20 μm length-ACNTs arrays were used, AuNPs were deposited mainly on the tips of the nanotubes (inset, Figure 3D). In this case, Fc-

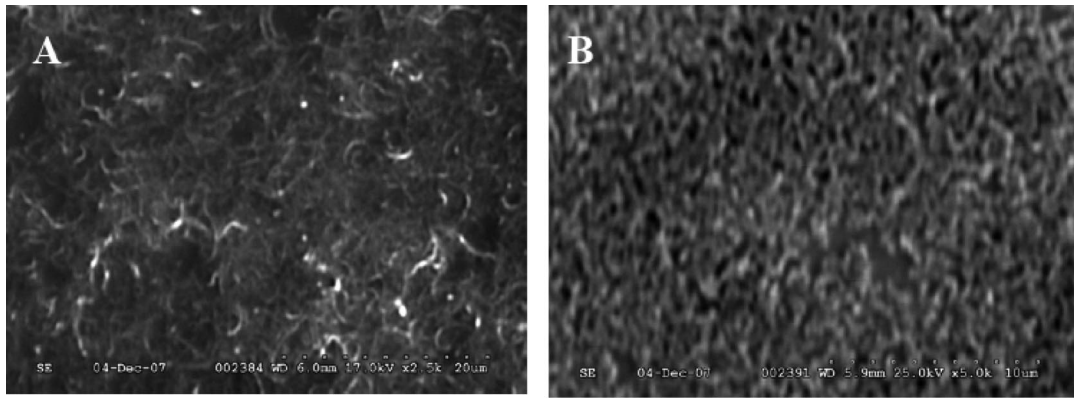

Figure 4. SEM images of (A) SWCNTs layer (2500×) dried upon 20 min of sonication in DMF and (B) SWCNTs layer (5000×) dried upon acid/peroxide treatment. SWCNTs after sonication in DMF treatment preserved their integrity. Bundled together they were about 5 μm long and distinct (A). In the second case, prolonged sonication in H_2SO_4/HNO_3 followed by H_2O_2/ H_2SO_4 treatment, neutralization, and filtering, led to significantly shorter SWCNTs with almost a granular structure. Electrodeposited AuNPs were not easily observable in the network of short SWCNTs.

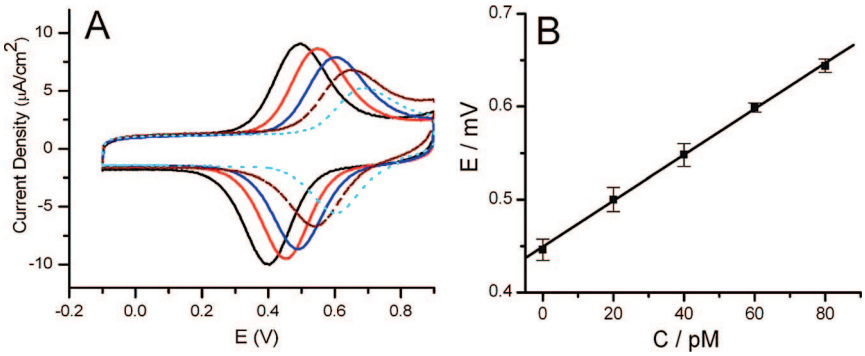

Figure 5. (A) Cyclic voltammograms of SWCNT/AuNP-modified gold electrodes: 0 pM (black, control), 20 pM (red), 40 pM (blue), 60 pM (brown), and 80 pM (cyan). Ag/AgCl was used as reference at 100 mV/s. (B) The linear relationship between HIV-1 PR concentration and the formal potential *E*°. Other conditions were as described in Figure 2.

pepstatin self-assembled on AuNPs, was distant from the electrode surface, resulting in poor electrochemical communication. The inset in Figure 3D shows AuNPs observable only at higher magnification (7000×). Only minimum bending of aligned CNTs was observed upon their rinsing under mild water stream (Figure 3B) and drying under an argon stream. The Au nanoparticle deposition process introduced additional stress but the nanotube array still consisted of individual tubes although with more bended morphology (Figure 3C). Peptide binding and protein adsorption exerted an additional pressure on the array and in turn, tubes were grouped together forming such an interesting pattern as shown in Figure 3D.

Significant improvement of the detection sensitivity was achieved by modification of the sensing probe with thiolated SWCNTs and gold nanoparticles. SWCNTs can be easily functionalized and decorated with a variety of inorganic nanomaterials including gold nanoparticles.[26] Thus, the resulting modified electrode was anticipated to improve the response to the binding event due to its higher exposed surface area. As compared with the only CNT modified surface (Figure 4A), the synergistic effect between AuNPs and the SWCNT integrated network (Figure 4B) facilitated electron transfer with the substrate. Functionalization of purified SWCNTs with thiol groups was realized, following the literature procedures[41] with slight modification as described in Experimental Section. Predispersed SWCNTs (10 μL) were coated on the gold electrode surface prior to the deposition of AuNPs. The high density of −SH groups allowed for electrochemical reduction of $AuCl_4^-$ to AuNPs at the side walls of SWCNTs. The formation of the SWCNT/AuNP composite was confirmed by SEM and Raman spectroscopy (Figure S2, Supporting Information). Figure 5 shows the change of the formal potential *E*° as a function of HIV-1 PR concentration. Under the optimized conditions, a linear range was obtained for all tested enzyme concentrations (*C*), starting from 0.5 pM. The linear regression equation was E (mV) = 0.458 + 0.00247C (C in pM) with a correlation coefficient of 0.998. The LOD for the target HIV-1 PR under the optimal conditions was 0.8 pM. This was ~1000-fold more sensitive than the level using the screen-printed electrode.[34] Detection reproducibility was determined from five different electrodes prepared under the same experimental conditions, with a relative standard deviation of 3.1% (n = 5). Hence, the signal amplification of the SWCNT-AuNP matrix resulted in a remarkable low detection limit where only SWCNT/AuNP could register the binding event at picomolar level (Figure 6A). In contrast, interactions with the Fc-pepstatin modified AuNP electrode composite were pronounced only with 1 nM of HIV 1-PR or higher. Therefore, this method might significantly improve the development of the inhibitory drug amount needed to suppress 50% of the PR activity *in vivo* (IC_{50}), which is still in the range of 10−30 nM.[42,43] Current efforts to design and screen for therapeutic protease inhibitors are being accelerated by the availability of structural information and several assay formats to screen, especially in the area of anticoagulation, neurodegenerative conditions, osteoporosis, type II diabetes, and rheumatoid arthritis. Therefore, our proposed detection scheme is expected to open up a new strategy for screening potent drugs for AIDS therapy or the detection of HIV-activity in infected T4 cells. Conceptually, protease when forming a complex with a potent inhibitor will no longer bind to the pepstatin-modified electrode and provoke no signal response.

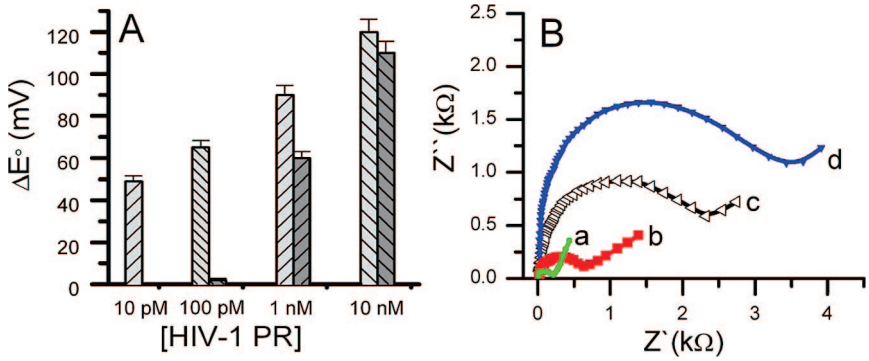

Figure 6. (A) The column chart showing the formal potential shift as a function of HIV-1 PR concentration for the two modified gold electrodes with SWCNT/ AuNP (light gray) and AuNP (dark gray). Error bars indicate the standard deviation (n = 5). (B) The Nyquist plot (Z_{im} *vs* Z_{re}) for electrochemical impedance measurement in the buffer medium, pH 7.4 containing 5.0 mM $Fe(CN)_6^{3-/4-}$ (1:1 mixture) as the redox probe at 0.24 V for (a) bare Au electrode, (b) the Fc-pepstatin-modified AuNP electrode, (c) the Au NP modified electrode after incubation with 1 nM HIV-1 PR, and (d) the peptide SWCNT/AuNP electrode after incubation with 10 pM HIV-1 PR. Frequency range: 0.1−100 kHz; ac amplitude, 5 mV. Other conditions are same as described in Figure 2.

A preliminary impedance analysis of the interfacial process (Figure 6B) demonstrated the simultaneous binding of HIV-1 PR with Fc-pepstatin that had bound to the SWCNT/AuNP or AuNP electrodes, as an indication of the surface binding events. The incubation of HIV-1 PR with the SWCNT/AuNP modified gold electrode drastically increased the electrochemical impedance, indicating an increased amount of HIV-1 PR was allowed to interact with the surface. This provides immediate evidence for the surface confinement of the SWCNTs, resulting in higher accessibility to the target enzyme. Notice that the experimental data of impedance can be further analyzed by using a model equivalent circuit, comprising a solution resistor, a charge-transfer resistance, a surface capacitance, and the impedance due to mass transfer of the redox species to the electrode described by the conventional Warburg.[37] This is a topic of future endeavors and beyond the scope of this work, that is, the development of simple cyclic voltammetry for detection of HIV-1 PR.

To assay the specificity of the proposed method, the electrochemical recognition of HIV-1 PR was tested in the presence of a large excess (5.1 mg/ml) of human serum albumin (HSA), the most abundant protein in human blood plasma. HSA normally constitutes about 60% of human plasma protein, and its concentration in blood plasma ranges from 3.5 to 5.0 mg/ml.[44] HSA only provoked a small decrease in i_{pa} and there was no change in $E°$. In contrast, a significant shift of $E°$ was observed only when 10 nM HIV-1 PR was spiked to the measurement solution (Figure 7). Similarly, human serum did not provoke any appreciable change in i_{pa} whereas 10 mM spiked human serum effected a comparable shift of $E°$ as observed for HSA (data not shown).

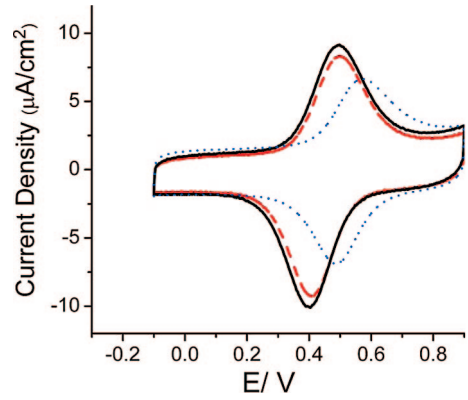

Figure 7. Cyclic voltammograms of the SWCNT/AuNP/Fc-pepstatin modified gold electrode in the presence of (——) assay buffer medium, (— — —) 75 μm HSA in the buffer solution, (... ... ...) 10 nM HIV-1 PR spiked in HSA, at 100 mV s^{-1}. Other conditions were as described in Figure 2.

We have demonstrated for the first time the combination of ferrocene-pepstatin with thiolated SWCNT/AuNP toward the construction of an extremely sensitive electrochemical detection method for HIV-1 PR at low picomolar levels. This proof of concept paves the way toward the development of an important tool for screening about 475 known putative proteases in the human genome or many disease states which manifest as altered protease expression and substrate proteolyzis are targets for therapeutic intervention. The generality of this approach can be easily extended to other protease/inhibitor pairs to expand the scope of using nanomaterials in biosensing.

EXPERIMENTAL SECITON

Materials. Human serum albumin (HSA), human male serum (AB), and HIV-1 PR recombinant expressed in *Escherichia coli* (25 μg) were purchased from Sigma. DTT (±threo-2,3-dihydroxy-1,4-butanedithiol) was obtained from Fluka. Fc-conjugated pepstatin (Cys-(NH-Pro_4-C(O)-Fc-C(O)-Val_2-Sta-Ala-Sta-OH)$_2$ was prepared as described in the literature.[34] Single walled carbon nanotubes (SWCNTs) (diameter of 1 nm, purity of CNTs > 90 wt %; length, 5−30 μm; specific surface area, 407 m^2/g; electrical conductivity, > 10^{-2} S/cm) were purchased from Carbon Nanotechnology (Houston, TX). Aligned carbon nanotube (ACNT) arrays (grown on Cr−Pt substrate, diameter 100−200 nm, length 20 μm, and density 10^9/cm^2) were obtained from Nano-Laboratory (Brighton, MA).

Preparation of ACNT/AuNP Electrodes. The plate containing the ACNT array was cut into 5 mm × 5 mm squares that were attached on a double-sided adhesive carbon tape. The other side of the C-tape was glued on plastic stripes (80 mm × 8 mm) to ensure the electrode rigidity. The 3 M (St. Paul, MN) insulating epoxy resin was carefully applied on the carbon so that only the ACNT array surface was exposed to the electrolyte for the electrochemical measurement. The epoxy layer solidified completely after 12 h in the oven at 40 °C. Electrodeposition of gold nanoparticles (NPs) on CNT arrays was performed by the potential-step technique from acidic solution of 0.5 M H_2SO_4 containing 5 mM $HAuCl_4$. The applied potential was stepped from 0.80 V (*vs* Ag/AgCl) to 0.20 V during 10 s. Such prepared electrodes were ready for electrochemical measurement and SEM analysis.

Pretreatment of SWCNTs. SWCNTs (30 mg) were first treated with a H_2SO_4/HNO_3 (3:1) mixture (10 mL) and sonicated for 10 h at 35 ± 5 °C. The resulting suspension was diluted with distilled water and filtered using a polycarbonate membrane with a pore size of 200 nm. The pH was adjusted to above 6 by subsequent rinsing with water. SWCNTs were suspended in a H_2O_2 (30 wt %, aq)/H_2SO_4 (4:1) mixture and refluxed for 3 h at 70 °C followed by sonication for 7 h to introduce carboxylic acid functional groups to the tubes. The same neutralization and filtration steps were followed. The oxidized and shortened SWCNTs were oven-dried and the powder was dissolved into absolute ethanol and treated with excess $NaBH_4$, and the resulting suspension was refluxed at 80 °C to reduce the carboxylic groups to hydroxyl groups. The reaction was then quenched by adding concentrated HCl dropwise until the excess of $NaBH_4$ disappeared. The suspension was then refluxed in thionyl chloride at 70 °C for 12 h followed by reflux in 3 M aq NaOH at 100 °C for 5 h. After dilution with distilled water, 1 M HCl was added dropwise until the neutral thiolated form was obtained, and the suspension was then filtered using a 200 nm pore-sized Teflon membrane filter. The remaining powder was washed three times with ethanol and oven-dried.

Electrode Preparation (AuNP-Modified Gold Electrode). Electrochemical deposition of gold nanoparticles on the gold disk electrode (3 mm in diameter, BAS) was performed in 0.5 M H_2SO_4 solution containing 5 mM $HAuCl_4$ using chronoamperometry at a constant potential. The electrode potential was stepped from an initial poten-

tial (E_i) of +0.8 V, where no reaction occurred, to +0.20 V, at which potential $AuCl_4^-$ was reduced to Au nanocrystals. The NP-modified electrode was then removed and rinsed with water and placed in the solution of 0.5 M H_2SO_4 for further measurements.

SWCNT/AuNP-Modified Gold Electrode. A 1 mg portion of the pretreated SWCNTs was redispersed into 2 mL of absolute ethanol and sonicated for 2 h to generate a black suspension. The prepolished gold electrode was coated with 10 μL of SWCNTs and allowed to dry under an argon stream. After rinsing, gold nanoparticles were then deposited electrochemically onto the SWCNT-modified electrode by following the same procedure as mentioned above. This would allow the thiolated SWCNTs to conjugate to gold-NPs through the stable Au−S bond. The modified electrodes were then rinsed thoroughly to remove unattached gold NPs and scanned in 0.5 M H_2SO_4 in the range of 0.1−1.2 V. The resulting electrodes were stable and could be stored for several days at room temperature without loosing their initial activity.

The peptide films were immobilized on SWCNT/NP electrodes using the published procedure.[33] In brief, the electrodes were immersed in ~1 mM thiol-terminated Fc-pepstatin conjugate prepared in 5% (by volume) acetic acid in ethanol for 12 h. A 20 nM HIV-1 PR stock solution was prepared in 0.1 M sodium acetate, pH 4.7, containing 2 mM EDTA, 1 mM DTT, and 10% DMSO was incubated at 23 °C for 1 h prior to the measurement. The activated enzyme was kept on ice. Subsequent dilutions of the enzyme were prepared by using the assay buffer. The peptide-modified electrodes were incubated with different HIV-1 PR concentrations for 1 h and washed twice with the assay buffer and deionized water. Control experiments were carried out with 75 μm HSA with and without HIV-1 PR.

Instrumentation. Cyclic voltammetry (CV), electrochemical impedance (EIS), and amperometric measurements were performed using an electrochemical analyzer coupled with a picoamp booster and Faraday cage (CHI 760B, CH Instruments, Austin, TX). A Pt wire (Aldrich, 99.9% purity, 1 mm diameter) and an Ag/AgCl, 3 M NaCl (BAS, West Lafayette, IN) electrode were used as counter and reference electrodes, respectively. Gold disk electrodes were polished with polishing paper (grid 2000) and subsequently with alumina until a mirror finish was obtained. The electrodes were sonicated for 5 min to remove the alumina residues followed by thorough rinsing with water and ethanol. The electrodes were then cleaned by cyclic voltammetry between 0 and +1.4 V *versus* Ag/AgCl at 100 mV s^{-1} in 0.5 M H_2SO_4 until a stable CV profile was obtained.

Scanning electron microscope (SEM) (Hitachi, S-2600 N, Tokyo, Japan) operating in high vacuum mode with an acceleration voltage of 10−24 kV and a working distance of 3−15 mm, depending on the sample, was used to analyze the morphology of CNT arrays and SWCNTs before and after different modification steps. Raman spectra were obtained by a Horiba/Jobin Yvon Laser Raman Analyzer (LabRAM HR800, Longjumeau, France) equipped with a frequency doubled argon ion 514 nm laser (Lexel 95-SHG) operating at 100 mW.

Acknowledgment. The authors are grateful to Prof. H.-B. Kraatz, University Western Ontario, London, ON, Canada, for his generous donation of the Fc-peptide conjugate, Y. Liu for obtaining Raman data, and K. B. Male of the Biotechnology Research Institute, National Research Council, Canada, for valuable discussion.

Supporting Information Available: SEM micrographs, Raman spectroscopy, and electrochemistry data. This material is available free of charge *via* the Internet at http://pubs.cas.org.

REFERENCES AND NOTES

1. Brik, A.; Wong, C. HIV-1 Protease: Mechanism and Drug Discovery. *Org. Biomol. Chem.* **2003**, *1*−*14*, 5–14.
2. Davies, D. R. T. The Structure and Function of the Aspartic Proteinases. *Annu. Rev. Biophys. Biophys. Chem.* **1990**, *19*, 189–215.
3. Jaskolski, M.; Tomasselli, A. G.; Sawyer, T. K.; Staples, D. G.; Heinrikson, R. L.; Schneider, J.; Kent, S. B. H.; Wlodawer, A. A. Structure at 2.5 Å Resolution of Chemically Synthesized Human Immunodeficiency Virus Type 1 Protease Complexed with a Hydroxyethylene-based Inhibitor. *Biochem.* **1991**, *30*, 1600–1609.
4. Nalam, M. N. L.; Ali, A.; Reddy, K.; Altman, M.; Chellappan, S.; Bandaranayake, R.; Anjum, S. G.; Rana, T. M.; Gilson, M. K.; Tidor, B.; et al. Circumventing Drug Resistance: Using the Substrate Envelope Hypothesis to Develop Robust Novel HIV-1 Protease Inhibitors. *Antiviral Ther.* **2007**, *12*, S138−S138.
5. Nalam, M. N. L.; Peeters, A.; Jonckers, T. H. M.; Dierynck, I.; Schiffer, C. A. Crystal Structure of Lysine Sulfonamide Inhibitor Reveals the Displacement of the Conserved Flap Water Molecule in Human Immunodeficiency Virus Type 1 Protease. *J. Virology* **2007**, *81*, 9512–9518.
6. Wainberg, M. A.; Clotet, B. Immunologic Response to Protease Inhibitor-Based Highly Active Antiretroviral Therapy: A Review. *Aids Patient Care Stand.* **2007**, *21*, 609–620.
7. Jayatilleke, P. R.; Nair, A. C.; Zauhar, R.; Welsh, W. J. Computational Studies on HIV-1 Protease Inhibitors: Influence of Calculated Inhibitor-Enzyme Binding Affinities on the Statistical Quality of 3D-QSAR CoMFA Models. *J. Med. Chem.* **2000**, *43*, 4446–4451.
8. Sham, Y. Y.; Chu, Z. T.; Tao, H.; Warshel, A. Examining Methods for Calculations of Binding Free Energies: LRA, LIE, PDLD-LRA, and PDLD/S-LRA Calculations of Ligands Binding to an HIV Protease. *Proteins* **2000**, *39*, 393–407.
9. Zhu, J.; Fan, H.; H, H. L.; Shi, Y. Structure-based Ligand Design for Flexible Proteins: Application of New F-Dyco Block. *J. Comput. Aided Mol. Des.* **2001**, *15*, 979–996.
10. Blair, I. S.; McDowell, D. A. Detection of Extracellular Proteinase of *Pseudomonas fragi* by Enzyme-Linked Immunosorbent Assay. *Curr. Microbiol.* **1995**, *31*, 180–185.
11. Frederiks, W. M.; Mook, O. R. F. Metabolic Mapping of Proteinase Activity with Emphasis on *in situ* Zymography of Gelatinases: Review and Protocols. *J. Histochem. Cytochem.* **2004**, *52*, 711–722.
12. Grant, S. A.; Weilbaecher, C.; Lichlyter, D. Development of a Protease Biosensor Utilizing Silica Nanobeads. *Sens. Actuators B* **2007**, *B121*, 482–489.
13. Hook, V. Y. H.; Schiller, M. R.; Nguyen, C.; Yasothornsrikul, S. Production of Radiolabeled Neuropeptide Precursors by *in vitro* Transcription and Translation. *Pept. Res.* **1996**, *9*, 183–187.
14. Ionescu, R. E.; Cosnier, S.; Marks, R. S. Protease Amperometric Sensor. *Anal. Chem.* **2006**, *78*, 6327–6331.
15. Orosco, M. M.; Pacholski, C.; Miskelly, G. M.; Sailor, M. J. Protein-Coated Porous Silicon Photonic Crystals for Amplified Optical Detection of Protease Activity. *Adv. Mater.* **2006**, *18*, 1393–1396.
16. Wegner, G. J.; Wark, A. W.; Lee, H. J.; Codner, E.; Saeki, T.; Fang, S.; Corn, R. M. Real-Time Surface Plasmon Resonance Imaging Measurements for the Multiplexed Determination of Protein Adsorption/Desorption Kinetics and Surface Enzymatic Reactions on Peptide Microarrays. *Anal. Chem.* **2004**, *76*, 5677–5684.
17. Williams, B. A.; Toone, E. J. Calorimetric Evaluation of Enzyme Kinetic Parameters. *J. Org. Chem.* **1993**, *58*, 3507–3510.
18. Eggeling, C.; Jaeger, S.; Winkler, D.; Kask, P. Comparison of Different Fluorescence Fluctuation Methods for Their Use in FRET Assays: Monitoring a Protease Reaction. *Curr. Pharm. Biotechnol.* **2005**, *6*, 351–371.
19. Eggeling, C.; Kask, P.; Winkler, D.; Jaeger, S. Rapid Analysis of Forster Resonance Energy Transfer by Two-Color Global Fluorescence Correlation Spectroscopy: Trypsin Proteinase Reaction. *Biophys. J.* **2005**, *89*, 605–618.
20. Gosalia, D. N.; Denney, W. S.; Salisbury, C. M.; Ellman, J. A.; Diamond, S. L. Functional Phenotyping of Human Plasma using a 361-Fluorogenic Substrate Biosensing Microarray. *Biotechnol. Bioeng.* **2006**, *94*, 1099–1110.
21. Kaufmann, S. H.; Mesner, P. W., Jr.; Martins, L. M.; Kottke, T. J. Methods used to Study Protease Activation during Apoptosis. In *Apoptosis in Neurobiology*, Hannun, Y. A., Boustany, R.-M., Eds.; CRC Press: Boca Raton, FL, 1999; pp 205−232.

22. Kohl, T.; Heinze, K. G.; Kuhlemann, R.; Koltermann, A.; Schwille, P. A. Protease Assay for Two-Photon Crosscorrelation and FRET Analysis based Solely on Fluorescent Proteins. *Proc. Natl. Acad. Sci. U.S.A.* **2002**, *99*, 12161–12166.
23. Pinto, M. R.; Schanze, K. S. Amplified Fluorescence Sensing of Protease Activity with Conjugated Polyelectrolytes. *Proc. Natl. Acad. Sci. U.S.A.* **2004**, *101*, 7505–7510.
24. Kilian, K. A.; Böcking, T.; Gaus, K.; Gal, M.; Gooding, J. J. Peptide-Modified Optical Filters for Detecting Protease Activity. *ACS Nano* **2007**, *1*, 355–361.
25. Azamian, B. R.; Coleman, K. S.; Davis, J. J.; Hanson, N.; Green, M. L. H. Directly Observed Covalent Coupling of Quantum Dots to Single-Wall Carbon Nanotubes. *Chem. Commun.* **2002**, *4*, 366–367.
26. Hrapovic, S.; Liu, Y.; Male, K. B.; Luong, J. H. T. Electrochemical Biosensing Platforms using Platinum Nanoparticles and Carbon Nanotubes. *Anal. Chem.* **2004**, *76*, 1083–1088.
27. Ellis, A. V.; Vijayamohanan, K.; Goswami, R.; Chakrapani, N.; Ramanathan, L. S.; Ajayan, P. M.; Ramanath, G. Hydrophobic Anchoring of Monolayer-Protected Gold Nanoclusters to Carbon Nanotubes. *Nano Lett.* **2003**, *3*, 279–282.
28. Wu, B.; Hou, S.; Yin, F.; Zhao, Z.; Wang, Y.; Wang, X.; Chen, Q. Amperometric Glucose Biosensor based on Multilayer Films *via* Layer-by-Layer Self-Assembly of Multi-wall Carbon Nanotubes, Gold Nanoparticles and Glucose Oxidase on the Pt Electrode. *Biosens. Bioelectron.* **2007**, *22*, 2854–2860.
29. Valentini, F.; Amine, A.; Orlanducci, S.; Terranova, M. L.; Palleschi, G. Nanotube Purification: Preparation and Characterization of Carbon Nnanotube Paste Electrodes. *Anal. Chem.* **2003**, *75*, 5413–5421.
30. Wang, J. Carbon Nanotube Based Electrochemical Biosensors: A Review. *Electroanalysis* **2005**, *17*, 7–14.
31. Castaneda, M. T.; Merkoic, A.; Pumera, M.; Alegret, S. Electrochemical Genosensors for Biomedical Applications based on Gold Nanoparticles. *Biosens. Bioelectron.* **2007**, *22*, 1961–1967.
32. Pumera, M.; Sanchez, S.; Ichinose, I.; Tang, J. Electrochemical Nanobiosensors. *Sens. Actuators B* **2007**, *123*, 1195–1205.
33. Mahmoud, K. A.; Kraatz, H.-B. A Bioorganometallic Approach for the Electrochemical Detection of Proteins: a Study on the Interaction of Ferrocene-Peptide Conjugates with Papain in Solution and on Au Surfaces. *Chem. Eur. J.* **2007**, *13*, 5885–5895.
34. Kerman, K.; Mahmoud, K. A.; Kraatz, H.-B. An Electrochemical Approach for the Detection of HIV-1 Protease. *Chem. Commun.* **2007**, *3829*, 3831.
35. Umezawa, H.; Aoyagi, T.; Morishima, H.; Matsuzaki, M.; Hamada, M. Pepstatin, a New Pepsin Inhibitor Produced by *Actinomycetes*. *J. Antibiot.* **1970**, *23*, 259–62.
36. Marciniszyn, J.; Hartsuck, J. A.; Tang, J. Mode of Inhibition of Acid Proteases by Pepstatin. *J. Biol. Chem.* **1976**, *251*, 7088–7094.
37. Li, C.-Z.; Liu, Y.; Luong, J. H. T. Impedance sensing of DNA binding drugs using gold substrates modified with gold nanoparticles. *Anal. Chem.* **2005**, *77*, 478–485.
38. Biebuyck, H. A.; Bian, C. D.; Whitesides, G. M. Self-organization of Organic Liquids on Patterned Self-assembled Monolayers of Alkanethiolates on Gold. *Langmuir* **1994**, *10*, 1825–1831.
39. Willey, T. M.; Vance, A. L.; Bostedt, C.; van Buuren, T.; Meulenberg, R. W.; Terminello, L. J.; Fadley, C. S. Surface Structure and Chemical Switching of Thioctic Acid Adsorbed on Au(111) as Observed using Near-Edge X-Ray Absorption Fine Structure. *Langmuir* **2004**, *20*, 4939–4944.
40. Miller, J. C.; Miller, J. N., Statistics for Analytical Chemistry. In *Ellis Horwood Series in Analytical Chemistry*, Chalmers, R. A., Masson, M., Eds.; Chichester, U.K., 1993; p 119.
41. Lim, J. K.; Yun, W. S.; Yoon, M.-H.; Lee, S. K.; Kim, C. H.; Kim, K.; Kim, S. K. Selective Thiolation of Single-walled Carbon Nanotubes. *Synth. Met.* **2003**, *139*, 521–527.
42. Cheng, Y.-S.; Lo, K.-H.; Hsu, H.-H.; Shao, Y.-M.; Yang, W.-B.; Lin, C.-H.; Wong, C.-H. Screening for HIV Protease Inhibitors by Protection against Activity-Mediated Cytotoxicity in *E. coli*. *J. Virol Methods* **2006**, *137*, 82–87.
43. Fuse, T.; Watanabe, K.; Kitazato, K.; Kobayashi, N. Establishment of a New Cell Line Inducibly Expressing HIV-1 Protease for Performing Safe and Highly Sensitive Screening of HIV Protease Inhibitors. *Microb. Infec.* **2006**, *8*, 1783–1789.
44. Peters, T. *All About Albumin: Biochemistry, Genetics, and Medical Applications*; Academic Press: San Diego, CA, 1996.